Water Interactions with Acetic Acid Layers on Ice and Graphite

- Panos Papagiannakopoulos,*,†,‡ Xiangrui Kong,† Erik S. Thomson,† and Jan B. C. Pettersson*,†
- †Department of Chemistry and Molecular Biology, Atmospheric Science, University of Gothenburg, SE-412 96 Gothenburg, Sweden
- ‡Department of Chemistry, Laboratory of Photochemistry and Kinetics, University of Crete, GR-71 003 Heraklion, Greece

Radha Gobinda Bhuin

25-10-14

Published in: Panos Papagiannakopoulos; Xiangrui Kong; Erik S. Thomson; Jan B. C. Pettersson; *J. Phys. Chem. B* Ahead of Print
DOI: 10.1021/jp503552w

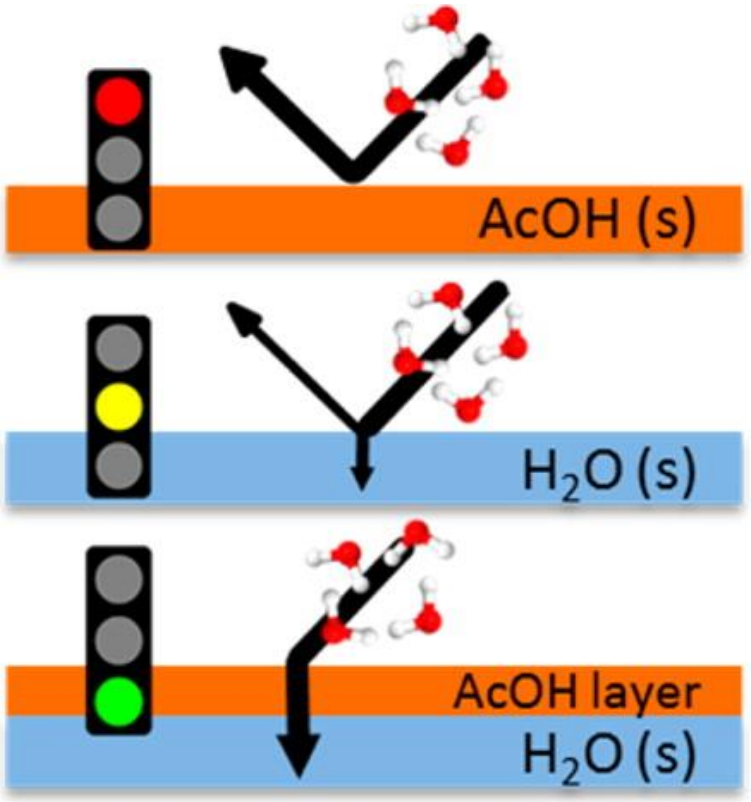

Published in: Panos Papagiannakopoulos; Xiangrui Kong; Erik S. Thomson; Jan B. C. Pettersson; *J. Phys. Chem. B* Ahead of Print
DOI: 10.1021/jp503552w

Introduction:

Condensation and evaporation of water are key processes in the endless movement of water and energy within the Earth system.

A multitude of organic compounds released to the atmosphere transform gas phase reactions into products with low vapor pressures that condense on existing aerosol and cloud particles.

Many reactions lead to the formation of carboxylic acids that are stable on the time scale of days or longer in the atmosphere.

Sources of atmospheric AcOH include primary emissions from soil, vegetation, and combustion processes including biomass burning.

AcOH plays an important role in tropospheric chemistry and atmospheric acidity.

Here they present results from EMB studies of water interactions with AcOH-covered surfaces with the overall aim of characterizing the dynamics and kinetics of the interactions.

Published in: Panos Papagiannakopoulos; Xiangrui Kong; Erik S. Thomson; Jan B. C. Pettersson; *J. Phys. Chem. B* Ahead of Print
DOI: 10.1021/jp503552w

Experimental Schematic:

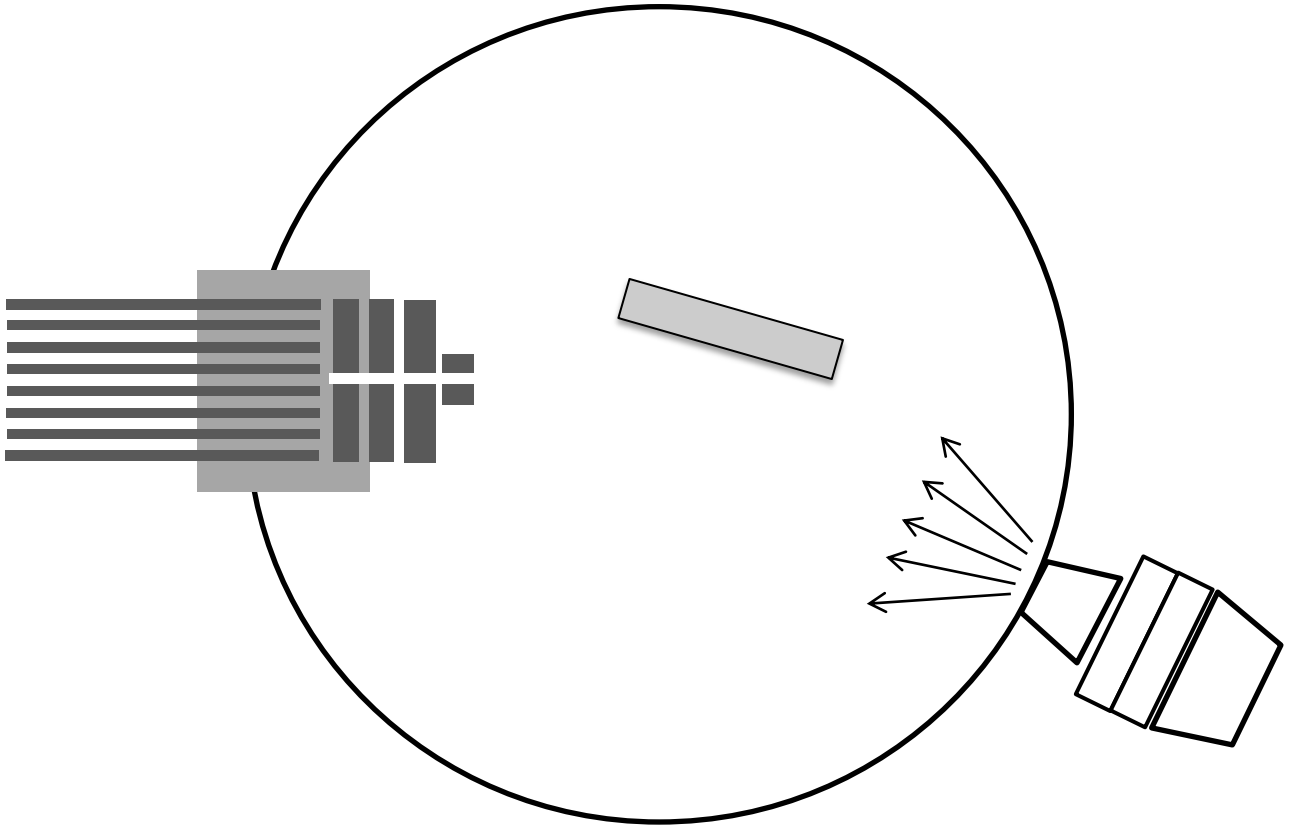

Published in: Panos Papagiannakopoulos; Xiangrui Kong; Erik S. Thomson; Jan B. C. Pettersson; *J. Phys. Chem. B* Ahead of Print
DOI: 10.1021/jp503552w

Analysis:

The TD is modeled as ordinary desorption, expressed in terms of measured intensity F_{res} as

$$F_{res} = C_1 e^{-kt} \quad (1)$$

where C_1 is a scaling factor, k is the desorption rate constant, and t is time. The inelastic scattering distribution is assumed to have the form[48]

$$I_{IS}(v(t)) = C_2 v(t)^4 \exp\left[-\left(\frac{v(t) - \overline{v}}{v_{IS}}\right)^2\right] \quad (2)$$

where C_2 is a scaling factor, $v(t)$ is the velocity calculated from t and the path length between the surface and the QMS, $\overline{v}$ represents the peak of the inelastically scattered velocities, and v_{IS} is

$$v_{IS} = \sqrt{\frac{2k_B T_{IS}}{m}} \quad (3)$$

where the temperature T_{IS} is a free fitting parameter that is indicative of the velocity spread of inelastically scattered particles, k_B is the Boltzmann constant, and m is the molecular mass.

, P_{TD} is computed as

$$P_{TD} = s_{graphite} I_{TD}^{AcOH} / I_{TD}^{graphite}$$

Published in: Panos Papagiannakopoulos; Xiangrui Kong; Erik S. Thomson; Jan B. C. Pettersson; *J. Phys. Chem. B* Ahead of Print
DOI: 10.1021/jp503552w

Results:

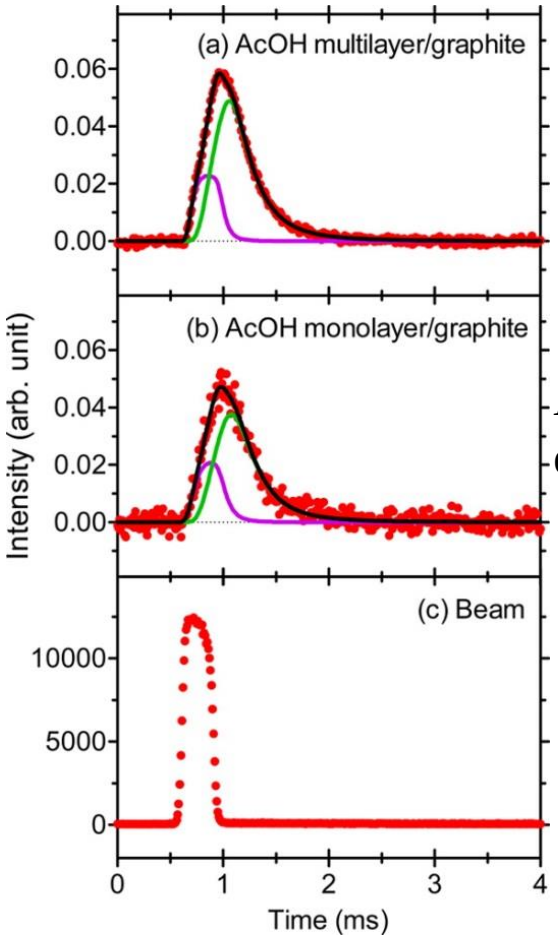

Final average kinetic energy of 6.1 ± 0.6 kJ mol^{-1}.

Absolute TD probability is determined to be 0.71 ± 0.07.

Absolute TD probability is determined to be 0.76 ± 0.07.

Time-of-flight distributions for D_2O inelastic scattering and thermal desorption from (a) solid AcOH and (b) an AcOH monolayer on graphite at 200 K. The time profile of the incident D_2O beam is shown in part c. The black, violet, and green curves show the total, inelastic, and thermal desorption components, respectively, obtained from the nonlinear least-squares data fitting as described in the text. The experimental data have been normalized to the incident beam intensity and smoothed with a seven-point stepwise average. The estimated equilibrium pressure P_0 over solid AcOH was 2×10^{-2} Pa.

Published in: Panos Papagiannakopoulos; Xiangrui Kong; Erik S. Thomson; Jan B. C. Pettersson; *J. Phys. Chem. B* Ahead of Print
DOI: 10.1021/jp503552w

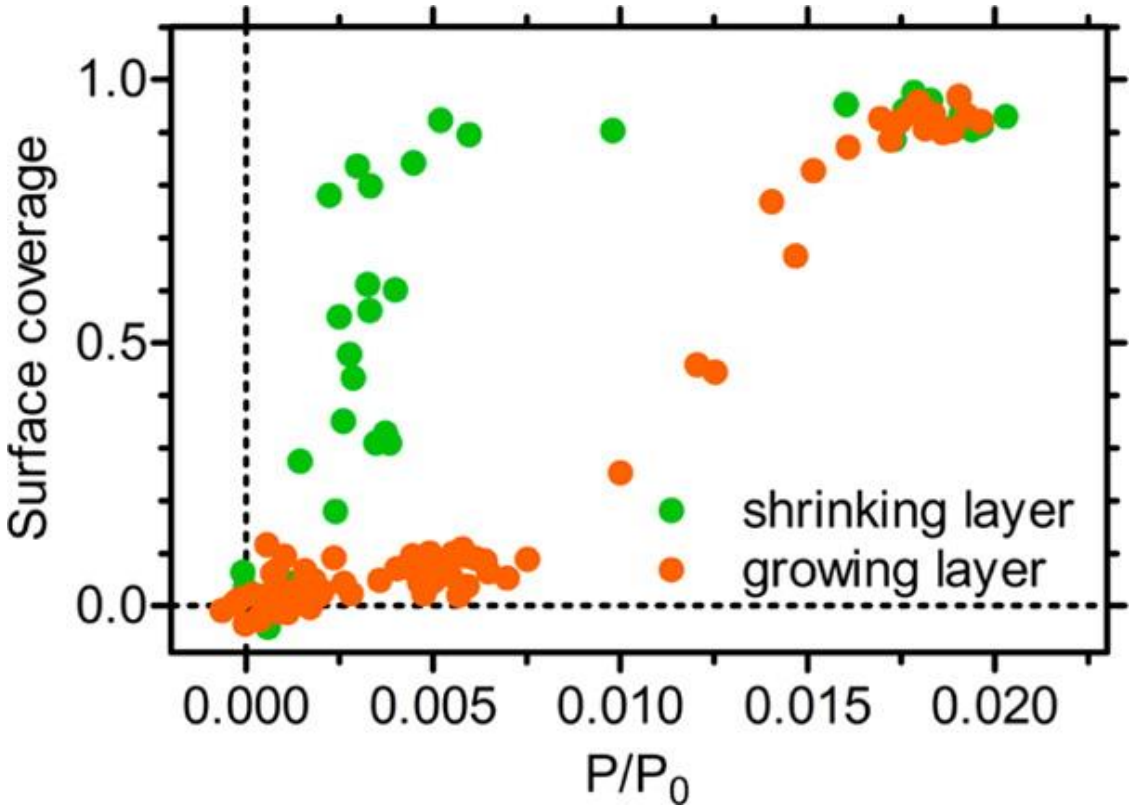

Submonolayer surface coverage of AcOH on graphite (T_s = 190 K) as a function of relative AcOH vapor pressure during layer growth (orange points) and shrinkage (green points). The equilibrium pressure $P_0 = 2 \times 10^{-3}$ Pa was experimentally determined by measuring the steady-state pressure over a μm-thick layer of pure AcOH.

Published in: Panos Papagiannakopoulos; Xiangrui Kong; Erik S. Thomson; Jan B. C. Pettersson; *J. Phys. Chem. B* Ahead of Print
DOI: 10.1021/jp503552w

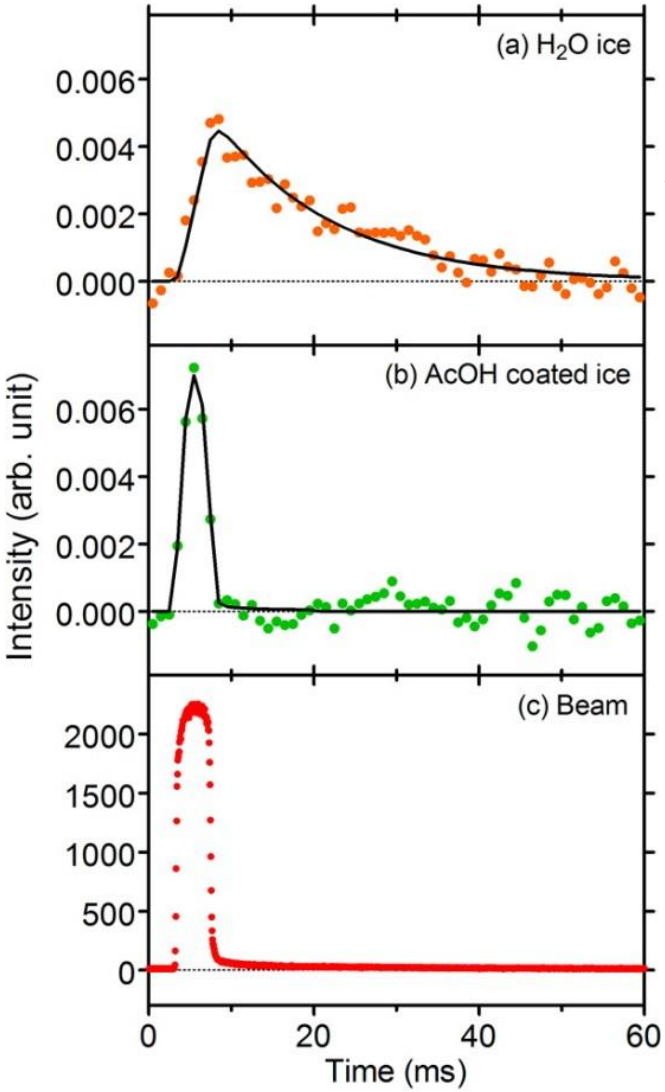

Accommodation coefficient 0.76 ± 0.07

Final average kinetic energy of 6.1 ± 0.6 kJ mol^{-1}.
Accommodation coefficient 1.00 ± 0.05.

Time-of-flight distributions for (a) pure thermal desorption of D_2O from pure ice and (b) pure inelastic scattering of D_2O from AcOH-covered ice surfaces, both at 186 K. The incident D_2O beam profile is shown in part c. The AcOH pressure was 1 × 10^{-4} Pa.

Published in: Panos Papagiannakopoulos; Xiangrui Kong; Erik S. Thomson; Jan B. C. Pettersson; *J. Phys. Chem. B* Ahead of Print
DOI: 10.1021/jp503552w

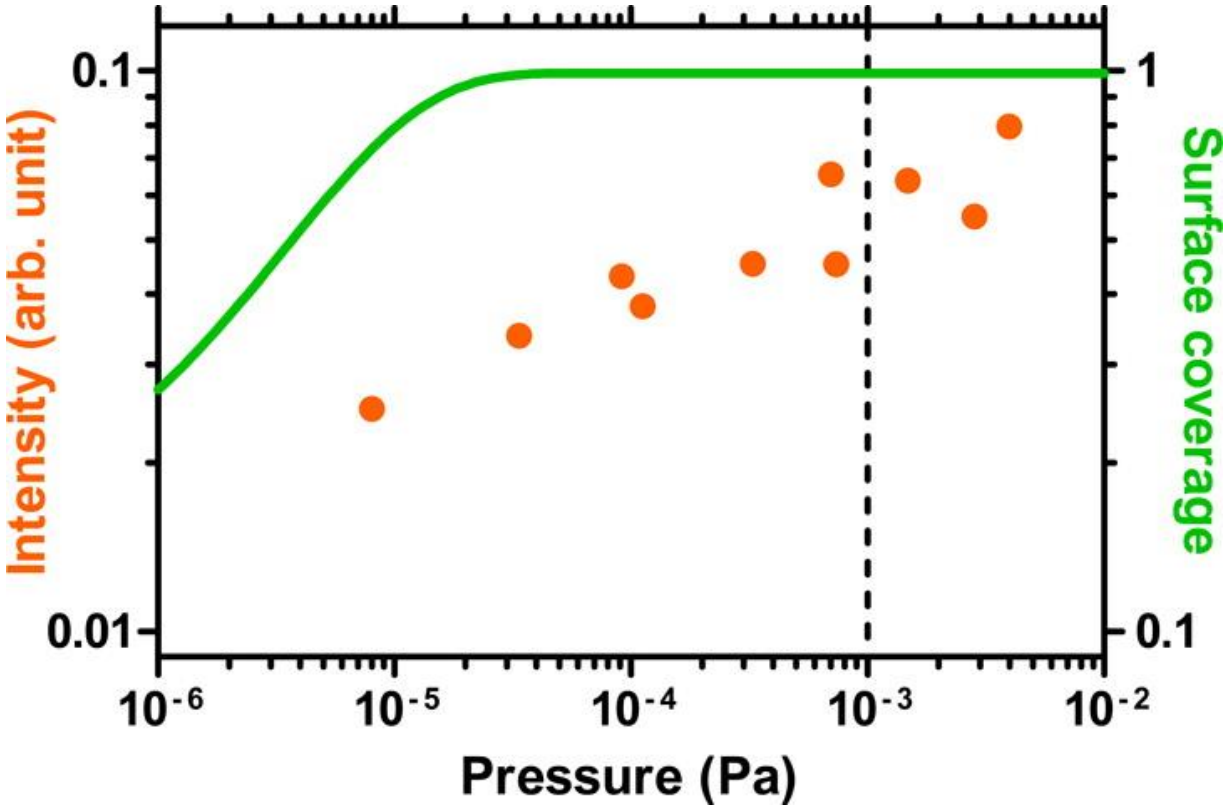

Relative intensity of D_2O inelastic scattering from AcOH-covered ice as a function of AcOH pressure (left axis) and the calculated surface coverage θ (right axis). The surface temperature was 186 K. The dashed line indicates the equilibrium pressure P_0 over pure AcOH.

Published in: Panos Papagiannakopoulos; Xiangrui Kong; Erik S. Thomson; Jan B. C. Pettersson; *J. Phys. Chem. B* Ahead of Print
DOI: 10.1021/jp503552w

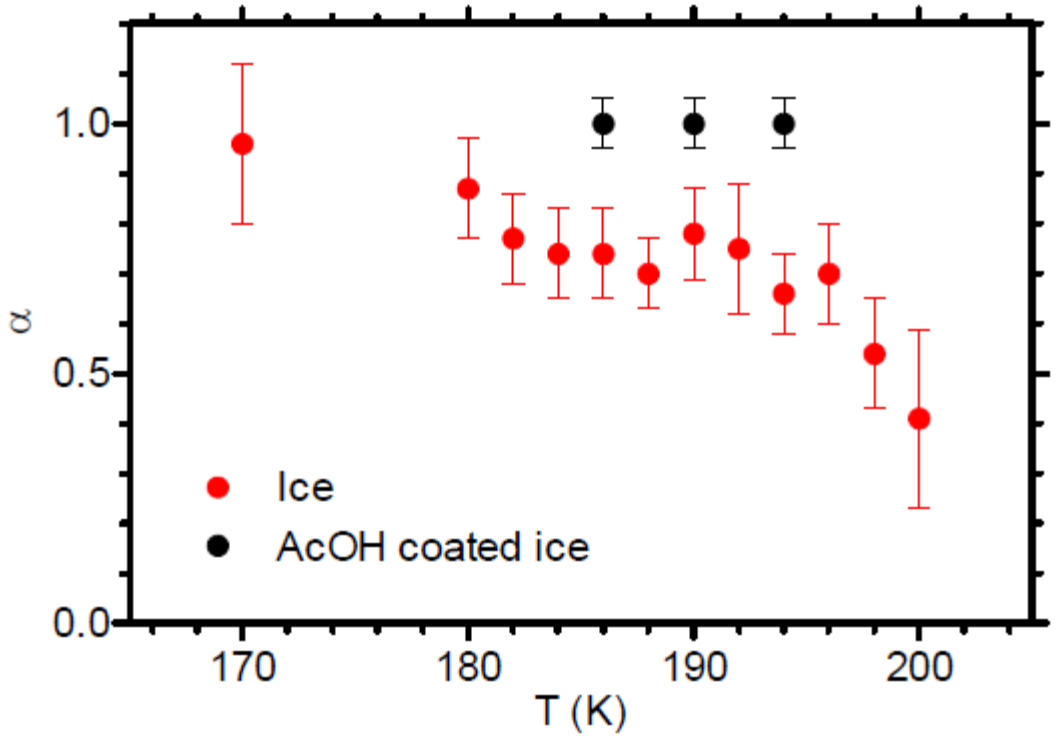

Comparison between the D_2O uptake coefficient $\alpha(T)$ on AcOH-covered (black points) and pure ice surfaces (red points) as a function of temperature.

Published in: Panos Papagiannakopoulos; Xiangrui Kong; Erik S. Thomson; Jan B. C. Pettersson; *J. Phys. Chem. B* Ahead of Print
DOI: 10.1021/jp503552w

Conclusion:

D_2O interactions with both bulk and monolayer AcOH on graphite and with AcOH-covered water ice using the EMB method have been studied.

Hyperthermal collisions of D_2O molecules with solid AcOH and with AcOH monolayers on graphite result in either inelastic scattering or trapping followed by rapid desorption (residence time <20 μs). This indicates that the AcOH surface has a closed surface structure with limited opportunities for water to form hydrogen bonds with surface molecule.

On water ice, adsorbed AcOH is observed to substantially alter the D_2O−surface interactions. A small fraction of incoming water molecules scatter inelastically from the AcOH layer, while trapped water molecules bind efficiently and remain on the ice surface on the time scale of the experiments (60 ms).

The behavior is qualitatively different from what is observed on the other AcOH surfaces studied herein, and on pure ice surfaces where a weakly bound precursor state limits bulk accommodation.

Published in: Panos Papagiannakopoulos; Xiangrui Kong; Erik S. Thomson; Jan B. C. Pettersson; *J. Phys. Chem. B* Ahead of Print
DOI: 10.1021/jp503552w

Thank you

Published in: Panos Papagiannakopoulos; Xiangrui Kong; Erik S. Thomson; Jan B. C. Pettersson; *J. Phys. Chem. B* Ahead of Print
DOI: 10.1021/jp503552w